

Accelerated warming of the Southern Ocean and its impacts on the hydrological cycle and sea ice

Jiping Liu¹ and Judith A. Curry

School of Earth and Atmospheric Sciences, Georgia Institute of Technology, Atlanta, GA 30332

Edited by Mark H. Thieme, University of California at San Diego, La Jolla, CA, and approved July 13, 2010 (received for review March 15, 2010)

The observed sea surface temperature in the Southern Ocean shows a substantial warming trend for the second half of the 20th century. Associated with the warming, there has been an enhanced atmospheric hydrological cycle in the Southern Ocean that results in an increase of the Antarctic sea ice for the past three decades through the reduced upward ocean heat transport and increased snowfall. The simulated sea surface temperature variability from two global coupled climate models for the second half of the 20th century is dominated by natural internal variability associated with the Antarctic Oscillation, suggesting that the models' internal variability is too strong, leading to a response to anthropogenic forcing that is too weak. With increased loading of greenhouse gases in the atmosphere through the 21st century, the models show an accelerated warming in the Southern Ocean, and indicate that anthropogenic forcing exceeds natural internal variability. The increased heating from below (ocean) and above (atmosphere) and increased liquid precipitation associated with the enhanced hydrological cycle results in a projected decline of the Antarctic sea ice.

sea surface temperature | precipitation | Antarctic sea ice

The Southern Ocean plays an important role in the Earth's climate system (1). The Southern Ocean is a significant sink for heat and CO₂, the world's most biologically productive ocean, and a site for the production of the coldest, densest water that is one of the dominant driving forces for the global overturning circulation. The strong westerly winds over the Southern Ocean drive the world's largest current system, the Antarctic Circumpolar Current (ACC, with a transport of ~135 Sv), which is the crossroads of the global ocean's water masses, connecting the Atlantic, Pacific, and Indian Oceans as well as connecting the deep ocean to the surface.

Although the Southern Ocean is critical to the Earth's climate system, detailed analyses of sea surface temperature (SST) variability have been hampered by limited observations (2–4). Comparisons of temperature profiles collected during the 1990s with profiles collected starting in the 1930s that were obtained from both ship-based hydrographic surveys and autonomous floats show that the upper 1,000 m of the Southern Hemisphere Ocean has warmed substantially (~0.2°C) during this time period, and that the warming is concentrated within the ACC (4). Modeling studies also indicate that the Southern Ocean might be undergoing rapid climate change. Climate model simulations of the National Center for Atmospheric Research (NCAR) for the 20th century that include anthropogenic forcing result in more rapid increases in SST and barotropic transport within the ACC in the south Atlantic, relative to the subtropical gyres to the north (5). If volcanic aerosols are not included, the simulated Southern Ocean warming in the climate model of the Canadian Centre for Climate Modeling and Analysis is nearly doubled, implying that the human impact on Southern Ocean warming is only partially realized at present (6).

In this study, we investigate the evolution of the spatial and temporal SST variability in the Southern Ocean using both observations and model simulations, and its impacts on the regional hydrological cycle and sea ice. The observed SST datasets used

here include the Hadley Centre Sea Ice and Sea Surface Temperature (HadISST) (7), and the extended reconstructed sea surface temperature (ERSST) (8). We confine the analysis to the period 1950–1999 due to large uncertainty associated with sparse in situ SST samplings in the Southern Hemisphere for the first half of the 20th century (9).

To increase confidence in the interpretation of simulated SST variability, we restrict our analysis to models that perform well in simulating the Southern Ocean climate: (i) the NCAR Community Climate System Model 3.0 (CCSM3), because the observed Antarctic Oscillation and sea ice variability is well represented in CCSM3 (10, 11), and (ii) the Geophysical Fluid Dynamics Laboratory Coupled Climate Model (GFDL-CM2.1), which has peak winds close to the observed latitude and a reasonable wind stress over the Southern Ocean, fed with the right amount and properties of the North Atlantic Deep Water, resulting in near-observed ACC transport (12). The experiments used here include: the preindustrial control experiment (PIctrl), the climate of the 20th century experiment (20C3M), and the 21st century climate projection experiments.

Results

Empirical Orthogonal Function (EOF) analyses performed on the area-weighted annual-mean observed SST south of 40°S for 1950–1999 show the first EOF mode of HadISST (Fig. 1A) having positive values extending from middle to high latitudes of the Southern Ocean, and negative values in the Antarctic and sub-Antarctic zones. The corresponding principle component (PC) (Fig. 2A) has a substantial upward trend (0.33 per decade, statistically significant at the 99% confidence level). The dominant spatiotemporal SST variability of ERSST is similar to that of HadISST (Fig. 1B and Fig. 2A). Thus, the observed SST pattern in the Southern Ocean during the second half of the 20th century is dominated by a broad-scale warming that accounts for one third of the total variance (28% for HadISST and 29% for ERSST). The strongest warming is found in the middle latitudes of the Southern Ocean, and the warming is reduced poleward. Because HadISST and ERSST use different data sources, analysis procedures, and historical bias corrections, the good agreement between them supports confidence in the analyzed Southern Ocean warming during the second half of the 20th century.

Fig. 1C shows the first EOF mode of the simulated SST for PIctrl of CCSM3. For PIctrl, there is no change in atmospheric composition (i.e., CO₂ is held constant at the preindustrial level), but it includes variations in solar and volcanic forcing and so simulates natural internal variability in response to natural external forcing. The leading EOF mode is characterized by an out-of-phase relationship between the middle and high latitudes, with

Author contributions: J.L. designed research, J.L. performed research, J.L. analyzed data, and J.L. and J.C. wrote the paper.

The authors declare no conflict of interest.

This article is a PNAS Direct Submission.

¹To whom correspondence should be addressed. E-mail: jliu@eas.gatech.edu.

This article contains supporting information online at www.pnas.org/lookup/suppl/doi:10.1073/pnas.1003336107/-DCSupplemental.

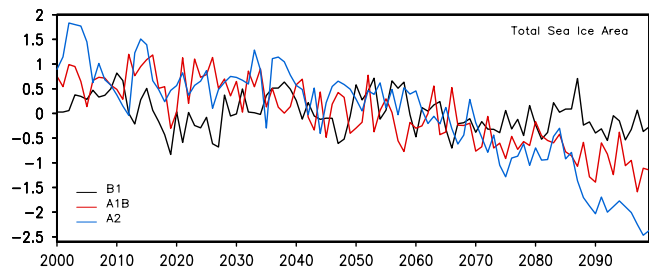


Fig. 5. Time series of the total Antarctic sea ice area anomaly ($\times 10^5$ km²) for the three scenarios during the 21st century.

ing to more absorbed solar radiation. Because of increased heating from below (ocean) and above (atmosphere), combined with increased liquid precipitation, the Antarctic sea ice is expected to decline in the 21st century. As shown in Fig. 5, all three scenarios show a loss of the total Antarctic sea ice area over the 21st century (0.4×10^5 km² per decade for B1, 2×10^5 km² per decade for A1B, and 3.02×10^5 km² per decade for A2), with the greatest loss occurring in the Atlantic and Indian sectors of the Antarctic. Additionally, the rate of decline accelerates after the late 2060s for the A1B and A2 scenarios. Thus, improved representation in models of atmosphere–sea ice–ocean interactions will be critical for forecasting Antarctic sea ice changes as climate warms.

Methods

The observed SST datasets used in the study include the Hadley Centre Sea Ice and Sea Surface Temperature (7), and the extended reconstructed sea surface temperature (8) for 1950–1999. Precipitation and evaporation obtained from the European Centre for Medium-Range Weather Forecast 40-Year Reanalysis* for 1958–1999, and Antarctic sea ice index obtained from the National Snow and Ice Data Center[†] are used to facilitate the analysis. We use model outputs from (i) the NCAR Community Climate System Model 3.0, and (ii) the Geophysical Fluid Dynamics Laboratory Coupled Climate Model, including the preindustrial control experiment, the climate of the 20th century experiment, and the 21st century climate projection experiments. We identify the dominant spatial and temporal patterns of SST variability in the Southern Ocean using EOF analysis. The EOF mode identifies regions that are closely related and with strong gradient (spatial variability), and the PC indicates the amplitude of EOF as it varies through time (temporal variability). Here, we focus on the first EOF modes that are statistically significant (24). We use the singular value decomposition analysis to identify the dominant coupled pattern between the ERA40's precipitation minus evaporation and HadISST SST south of 40°S for 1958–1999.

ACKNOWLEDGMENTS. We thank the Program for Climate Model Diagnosis and Intercomparison for collecting and archiving model outputs for the Fourth Assessment of the Intergovernmental Panel on Climate Change. This research was supported by the National Science Foundation Polar Programs (0838920) and National Aeronautics and Space Administration (NASA) Energy and Water Cycle Study (NEWS).

[†]<http://nsidc.org/data/g02135.html>

1. Mayewski PA, et al. (2009) State of the Antarctic and Southern Ocean climate system. *Rev Geophys* 47:RG1003 doi: 10.1029/2007RG000231.
2. Hegerl GC, Bindoff NL (2005) Warming of the world's oceans. *Science* 309:254–255.
3. Levitus S, Antonov JL, Boyer TP (2005) Warming of the world ocean, 1955–2003. *Geophys Res Lett* 32:L02604 doi: 10.1029/2004GL021592.
4. Gille S (2008) Decadal-scale temperature trends in the Southern Hemisphere Ocean. *J Climate* 21:4749–4765.
5. Wainer I, Taschetto A, Otto-Bliesner B, Brady E (2004) A numerical study of the impact of greenhouse gases on the South Atlantic Ocean climatology. *Climatic Change* 66:163–189.
6. Fyfe JC (2006) Southern Ocean warming due to human influence. *Geophys Res Lett* 33 doi: 10.1029/2006GL027247.
7. Rayner NA, et al. (2003) Global analyses of sea surface temperature, sea ice, and night marine air temperature since the late nineteenth century. *J Geophys Res* 108 doi: 10.1029/2002JD002670.
8. Smith TM, Reynolds RW (2004) Improved extended reconstruction of SST (1854–1997). *J Climate* 17:2466–2477.
9. Smith TM, Reynolds RW (2003) Extended reconstruction of global sea surface temperatures based on COADS data (1854–1997). *J Climate* 16:1495–1510.
10. Raphael M, Holland M (2006) Twentieth century simulation of the southern hemisphere climate in coupled models. Part I: Large scale circulation variability. *Clim Dynam* 26:217–228.
11. Holland M, Raphael M (2006) Twentieth century simulation of the southern hemisphere climate in coupled models. Part II: Sea ice conditions and variability. *Clim Dynam* 26:229–245.
12. Russell JL, Souffer RJ, Dixon KW (2006) Intercomparison of the Southern Ocean Circulations in the IPCC Coupled Model Control Simulations. *J Climate* 19:4560–4575.
13. Thompson DWJ, Wallace JM (2000) Annular modes in the extratropical circulation. Part I: Month-to-month variability. *J Climate* 13:1000–1016.
14. Hall A, Visbeck M (2002) Synchronous variability in the Southern Hemisphere atmosphere, sea ice, and ocean resulting from the annular mode. *J Climate* 15:3043–3057.
15. Sen Gupta A, England MH (2006) Coupled ocean-atmosphere-ice response to variations in the Southern Annular Mode. *J Climate* 19:4457–4486.
16. Ciasto LM, Thompson DWJ (2008) Observations of large-scale ocean–atmosphere interactions in the Southern Hemisphere. *J Climate* 21:1244–1259.
17. Bretherton CS, Smith C, Wallace JM (1992) An intercomparison of methods for finding coupled patterns in climate data. *J Climate* 5:541–560.
18. Wong APS, Bindoff NL, Church JA (1999) Large-scale freshening of intermediate waters in the Pacific and Indian Oceans. *Nature* 400:440–443.
19. Boning CW, Dispert A, Visbeck M, Rintoul SR, Schwarzkopf FU (2008) The response of the Antarctic circumpolar current to recent climate change. *Nat Geosci* 1:864–869.
20. Zhang J (2007) Increasing Antarctic sea ice under warming atmospheric and oceanic conditions. *J Climate* 20:2515–2529.
21. Liu J, Curry JA, Martinson DG (2004) Interpretation of recent Antarctic sea ice variability. *Geophys Res Lett* 31:L02205 doi: 10.1029/2003GL018732.
22. Cavalieri DJ, Parkinson CL (2008) Antarctic sea ice variability and trends, 1979–2006. *J Geophys Res* 113:C07004 doi: 10.1029/2007JC004564.
23. Yin JH (2005) A consistent poleward shift of the storm tracks in the simulations of 21st century climate. *Geophys Res Lett* 32:L18701 doi: 10.1029/2005GL023684.
24. North GR, Bell TL, Chalan RF, Moeng FJ (1982) Sampling errors in the estimation of empirical orthogonal functions. *Mon Weather Rev* 110:699–706.